Separation of the Electromyographic from the Electrocardiographic Signals and Vice Versa. A Topical Review of the Dynamic Procedure

Ivaylo Christov[1*], Atanas Gotchev[2], Giovanni Bortolan[3], Tatyana Neycheva[1], Rositsa Raikova[1], Ramun Schmid[4]

[1]*Institute of Biophysics and Biomedical Engineering*
Bulgarian Academy of Sciences, Sofia, Bulgaria
E-mails: Ivaylo.Christov@biomed.bas.bg, tatiana@biomed.bas.bg, rosi.raikova@biomed.bas.bg

[2]*Tampere University of Technology*
Tampere, Finland
E-mail: atanas.gotchev@tuni.fi

[3]*Institute of Neuroscience – National Research Council*
IN-CNR, Padova, Italy
E-mail: giovanni.bortolan@isib.cnr.it

[4]*Signal Processing, Schiller AG*
Baar, Switzerland
E-mail: Ramun.Schmid@schiller.ch

[*]*Corresponding author*

Received: November 20, 2019 **Accepted: March 26, 2020**

Published: September 30, 2020

Abstract: *Electrocardiographic (ECG) and electromyographic (EMG) signals are inevitably and simultaneously recorded from the same electrodes and are respectively useful signal and noise in electrocardiography, and vice versa in electromyography. The frequency domains of the two signals overlap, making it difficult to filter the noise without distortion of the useful signal.*

An original 'dynamic method' for separation of the two signals was created. In a series of publications that began in 1999 with filtering of EMG noise from ECG signal, we have described the method and have made a number of improvements such as noise analysis and automatic on/off triggering in presence/absence of noise, online application, and tuning the parameters, to fulfill the last filtering recommendations of the American Heart Association.

No matter if the Dynamic procedure is to be used in electrocardiography or in electromyography, the method contains the following: (i) Evaluation of the frequency bands of the ECG signal; (ii) filtering (suppression) of the EMG signal by dynamic change of the size of the filtering window for maximal preservation of the morphology of the ECG waves. The cutoff frequency is individual for any signal sample and varies from 13 Hz at the linear segments of the ECG signal, trough 25 Hz for the T-waves of high amplitude, and up to 400 Hz for the QRS-complexes; (iii) EMG signal separation by subtraction of the filtered ECG signal from ECG + EMG initial signal.

With the current review, we are attempting to summarize all done over the years on the Dynamic procedure.

Keywords: *Electrocardiography, Electromyography, Dynamic filtration, High frequency noise, Wings function.*

Introduction

Electrocardiographic (ECG) and electromyographic (EMG) signals are simultaneously and inevitably recorded from the same electrodes and are respectively useful signal and noise in electrocardiography, and vice versa in electromyography.

In electromyography, ECG noise superimposes the EMG signal when some of the investigated muscles are trunk muscles and especially for those ones placed on the left. The noise obstructs the EMG analysis and makes impossible the control of technical devices as ortheses, exoskeletons, prosthesis, etc. [1, 2].

The frequency domains of the ECG and EMG signals overlap, making it difficult to filter the noise without distortion of the useful signal. The energy of the EMG signals is in the frequency range from 0 to 500 Hz [3], and the useful information is contained within the range 10-400 Hz [4]. For that reason, the 30 Hz high-pass 4^{th} order Butterworth filter recommended in [5] will cut useful information between 10 and 30 Hz and will not filter the high-frequency components of the ECG signal thus destroying the EMG signal.

Considering the fact that ECG and EMG signals superimpose linearly, Sbrollini at al. [6] applied their Segmented-Beat Modulation Method for signal separation providing first the ECG signal, and then the EMG signal by subtraction.

The success of ECG signal removing from the mixed EMG + ECG signals depends on the amplitude ratio between these two signals. Butterworth high-pass filter with cut-off frequency of 30 Hz and order of 4 will not be successful, when these two amplitudes are equal or when the amplitude of the ECG signal is higher than the amplitude of the EMG signal [7]. Lu et al. [8] used adaptive filter in removing ECG interference from surface EMG signal recorded from the trapezius muscles of patients with cervical dystonia. The efficiency of their method decreased with reducing the signal-to-noise ratio (SNR), but it still achieved respectable performance even when the SNR is below −5 dB.

Zhou et al. [9] aimed to remove ECG artifacts in real time for myoelectric prosthesis control, a clinical application that demanded speed and time-linearity of the used methods. The authors investigated the removal of ECG artifacts by high frequency pass filters and by adaptive spike clipping, with no specific quantification of the ECG removal.

Abbaspour and Fallah [10] removed ECG noise from EMG signal by adaptive subtraction, with a low pass filtering of an averaged ECG template.

Christov et al. suggested ECG-noise removal from EMG-signal to be done by subtraction of hybrid template of averaged PQRS-T [11]. Special care is taken, the ectopic beats to be excluded from the averaging.

In electrocardiography, EMG noise in resting ECG signal is quite common in subjects with uncontrollable tremor, in disabled persons having to exert effort in maintaining a position of their extremities or a body posture, in children, etc. The EMG noise can make it difficult to localize automatically the ECG waves and obstructs the visual analysis.

Most of the ECG diagnostic information is contained below 100 Hz in adults, although low-amplitude, high-frequency components as high as 500 Hz had been detected and studied [12]. Setting the low-pass filter of the ECG signal to a low cutoff level eliminates not only the

muscle EMG noise but also the clinically significant high-frequency components of the signals inside the QRS complex [13, 14], J-waves [15] and pacemaker spikes [14]. For that reason, the American Heart Association (AHA) changed its low-pass filter recommendation from 35 Hz cutoff in 1967 [16], to 150 Hz for adolescents and adults, and to 250 Hz for children in 2007 [12].

Low-pass filtering with 35 Hz cut-off frequency is presented in Fig. 1. The filter distorts the high-frequency components of the QRS (shown by arrows). This is expressed by strong reduction of the QRS amplitude, in the first example, and almost full suppression of the QRS fragmentation (essential predictor of mortality and sudden cardiac death [17]), in the second example.

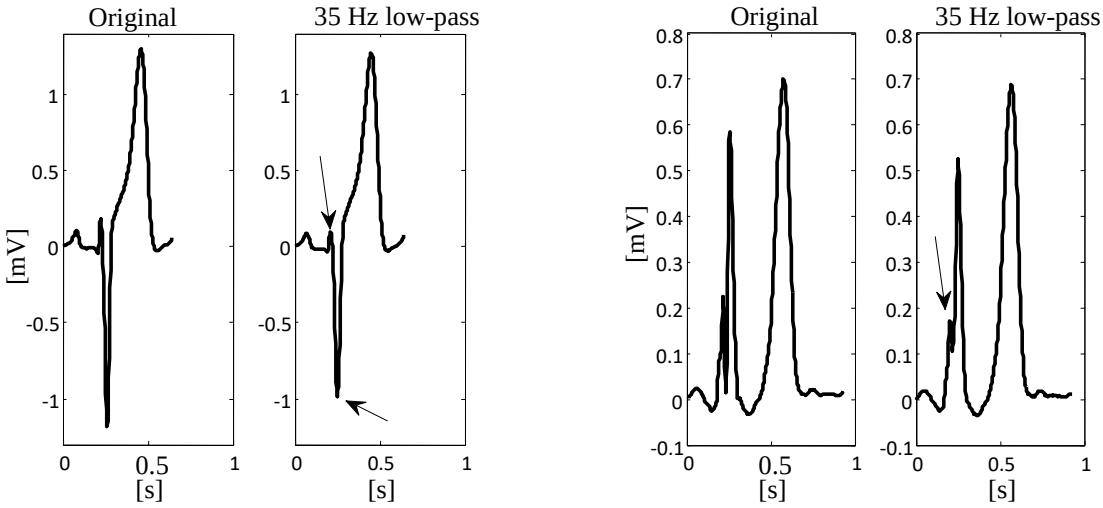

Fig. 1 Two ECG signals filtered with a cutoff frequency of 35 Hz

In the clinical practice, little attention tends to be paid to the filter setting of the ECG instruments, resulting in inappropriate filter application. In fact, Kligfield and Okin [18] found that the low-pass filter setting was 100 Hz and above in 25% of the ECG devices and less than 100 Hz (most commonly 40 Hz) in 75% of the ECG devices obtained within an American medical community.

The tendency of maximal preservation of the QRS high-frequency components and filtering with a cutoff frequency of higher than 50 Hz [18] leads to a high level of residual noise. This is shown in Fig. 2, where an original ECG signal containing EMG noise is filtered with 35 Hz, 150 Hz and 250 Hz cutoff frequencies respectively.

The presence of EMG noise could cause serious problems to the analysis of the signal out of QRS and will worsen the T-end localization, detection of ischemia (in the ST interval), atrial fibrillation and flutter (in the PQ interval), detection of T-wave alternans, etc.

Sayyad and Mundada [19] were using extended Kalman filter and extended Kalman smoother. Priority was given to the smoother, but in both methods, a great signal distortion was observed in the QRS.

Rakshit and Das [20] proposed, an efficient ECG denoising method using combined empirical mode decomposition and adaptive switching mean filter. Minimum distortion was achieved by restoration of the R-peaks, attenuated by the mean filter.

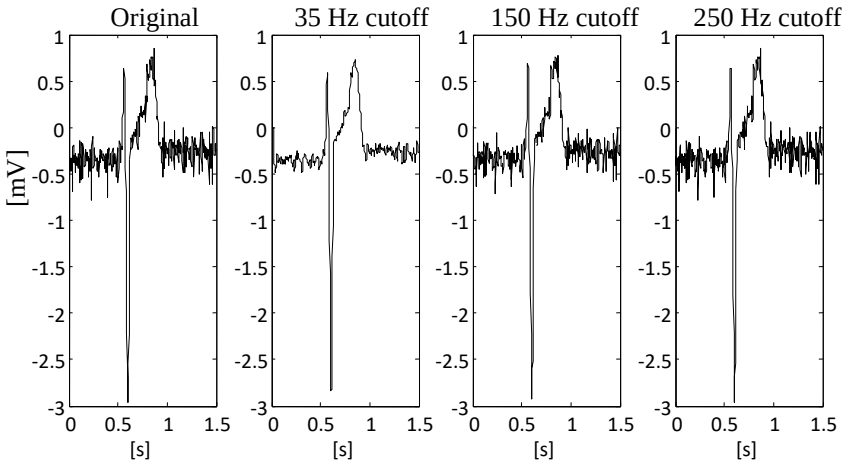

Fig. 2 An ECG signal containing EMG noise,
filtered with 35 Hz, 150 Hz and 250 Hz cutoff frequencies

Dotsinsky and Mihov [21] were filtering the noise in three steps: (i) Moving averaging with first zero set at 50 Hz to suppress tremor and powerline interference simultaneously; (ii) The reduced peaks of QRS complexes were restored by a procedure called linearly-angular; (iii) Finally, a Savitzky-Golay smoothing filter was applied for supplementary tremor suppression outside the QRS complexes. In another study they aimed to develop simple approach for tremor suppression using heuristic relations between the ECG waves and parameters of some types of comb filters applied specifically on selected parts of the signal [22]. The heuristic relations are performed with appropriate criteria that determine comb filters.

Joy and Manimegalai [23] were using wavelet transform to remove the EMG noise. The proposed method selected the best suitable wavelet function based at the 5^{th} decomposition level. The authors claimed that the method retains the distinctive features of the ECG signal.

Myriad filters are known to perform well with Gaussian and impulsive noise. Tulyakova [24, 25] presented good results with locally-adaptive, low-pass Myriad filters for ECG processing.

An example of dynamic filtering is present in De Pinto [26], where a time-varying low pass filter was used , maximizing (minimizing) the bandwidth inside (outside) the QRS complex.

It is difficult to identify comparable review papers in the literature on EMG noise filtration from ECG signal. Kalra et al. [27] and Luo and Johnston [28] consider the problem to minimize the EMG noise from ECG signal with different methods: Wavelets, Principal Component Analysis, Independent Component Analysis, Low-pass filters. Both materials give common and basic knowledge about existing filters and the topic of suppression of muscle noise is not deeply treated.

'Dynamic' procedure for separation of the two signals – ECG and EMG was developed [29] and build up further [30-37]. The considered procedure produces specific individual filtering coefficients for every single sample of the signal, in an attempt to satisfy in the best possible way the conflicting requirements for a strong suppression of noise, and at the same time for a maximal preservation of the useful signal.

Methods

Electrocardiography

Dynamic control

The dynamic control was evaluated in two ways: by the frequency bands of the ECG waves and by the amount of filtered noise inside and outside the QRS-complex.

Evaluation of the frequency bands of the ECG waves

Evaluation of the frequency bands of the ECG elements was on the basic of the Dynamic filtration. A so-called '***Wings***' function criterion was created [29], which allowed a dynamic application with different filtering rate of the approximation procedure of Savitzky and Golay [41]. Evaluation of the frequency spectra of the ECG waves is shown in Fig. 3. It consists of:

- filtering of the initial ECG signal (Fig. 3a) to eliminate/suppress power-line interference and EMG noise. The goal is a complete suppression of the noises, no matter of the high frequency distortion occurring in amplitude reduction of the QRS, as shown in subplot (b) of Fig. 3;
- performing of the '***Wings***' function (details are given later on), which reacts with sharp peaks to the steep slopes of the QRS and high amplitude T-waves (Fig. 3c – traced with thin line);
- filtering of the '***Wings***' to smooth the peaks (Fig. 3c – traced with thick line);
- transfer of the particular values of the '***Wings***' function to a window length '***wl***' (Fig. 3d), over which the final Savitzky-Golay filter (SGF) will be applied.

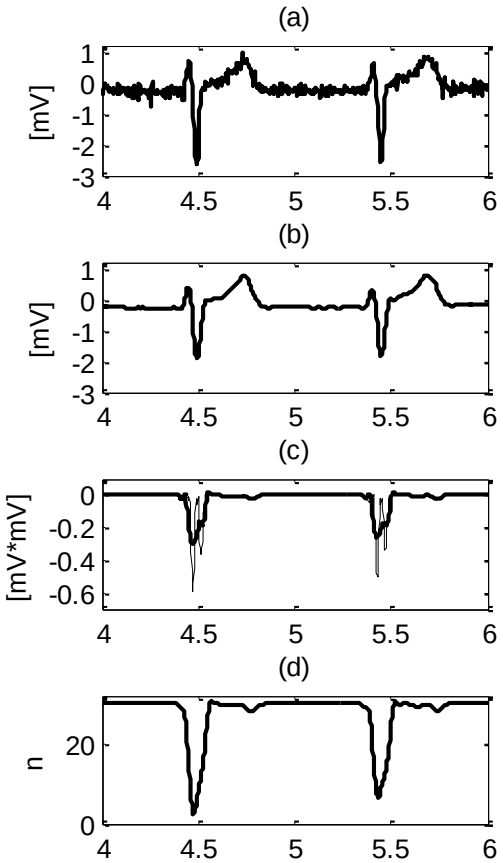

Fig. 3 Evaluation of the frequency response of ECG waves:
(a) ECG signal; (b) filtered ECG signal; (c) '***Wings***' function;
(d) transfer the '***Wings***' into dynamic window length '***wl* = *-n*:*n***' of the SGF.

Block diagrams describing two methods for evaluation of the frequency spectra of the ECG waves [29 and 33] are shown in Fig. 4 and Fig. 5, respectively.

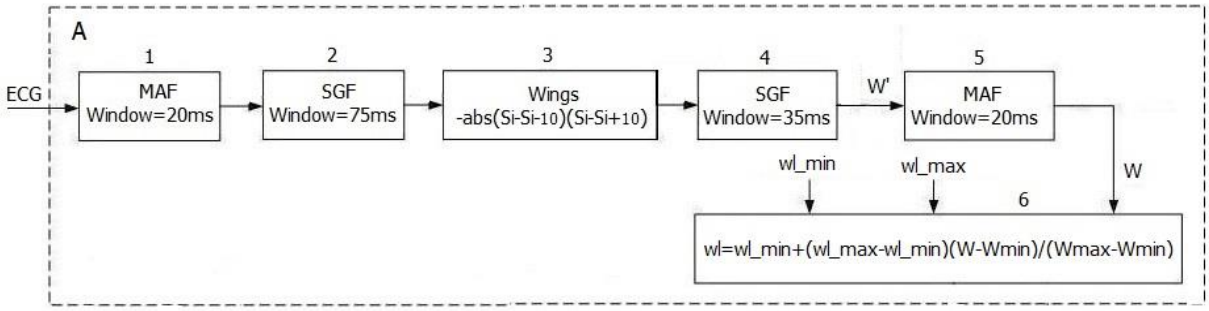

Fig. 4 Block diagram of the evaluation of window length of SGF filer through frequency bands of the ECG signal [29]

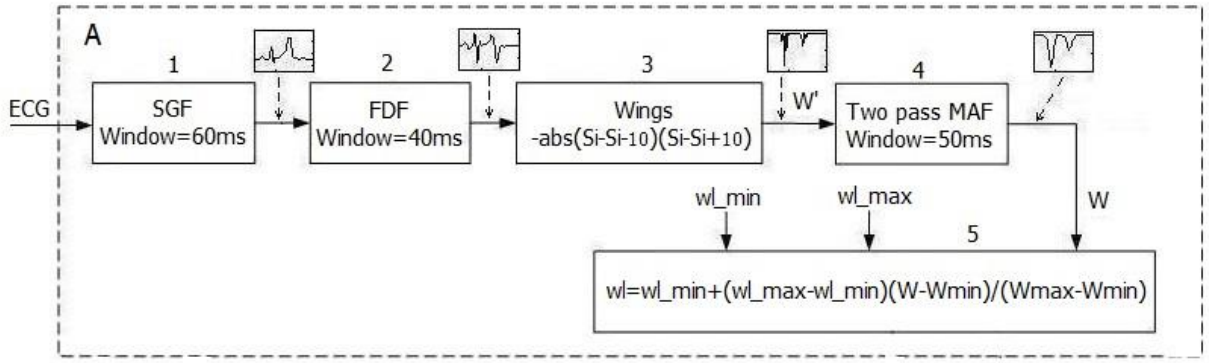

Fig. 5 Block diagram of the evaluation of window length of SGF filer through frequency bands of the ECG [33]

Worsening of the EMG suppression at high EMG noise and high baseline drift was observed during the years, using the method described in the first publication ([29], Fig. 4). For that reason the method of Christov et al. [33] was with increased filtering ability in the pre-'***Wings***' stage (Fig. 5).

Three filters were used in evaluation of the frequency bands of the ECG [33]. SGF (block 1 of Fig. 5) will be described in a special chapter. Moving averaging filter, (MAF – block 4 of Fig. 5) has first zero at 20 Hz for a window of 50 ms. First difference filter (FDF – block 2 of Fig. 5) has a transfer function of

$$T_{FDF}(z) = \frac{1 - z^m}{2}, \tag{1}$$

where FDF is a comb filter with first zero frequency $\boldsymbol{f = 1/(mT_S)}$. We selected $\boldsymbol{m}$ to be

$$m = \frac{2T_{PL}}{T_S}, \tag{2}$$

where $\boldsymbol{T_{PL}}$ is the period of the power line interference, and $\boldsymbol{T_S}$ is the sampling interval. The high-pass FDF of 3 dB is set at about 6 Hz frequency, and the higher frequency notches reject all harmonics of power-line interference.

The cut-off frequency of SGF for a window of 60 ms is *Fc* = 12 Hz. By a window of 40 ms (difference between two samples, 40 ms apart), FDF is tuned to pass at the same frequency bandwidth of 6-18 Hz.

Power-line frequency instability (not precise 50 Hz but 49 Hz, for example, see Eq. (2)) would slightly worsen the FDF functionality, but with no effect to the final result, since the power-line interference is filtered twice: by SGF and by FDF.

A so-called '***Wings***' function was found by multiplying the slopes of two adjacent segments of 10 ms length having a common central point. The product absolute value was then taken and inverted (block 3 of Fig. 3). For a 1000 Hz sampling rate the '***Wings***' function is:

$$Wings_i = -abs\left(\left(S_i - S_{i-10}\right) - \left(S_i - S_{i+10}\right)\right), \text{ for } i > 10. \quad (3)$$

The segment length of 10 ms was chosen in order to obtain a certain level of signal smoothing in the process of frequency response evaluation. We have found that this value was not particularly critical, as a smaller interval results in more varying '***Wings***' function and thus stronger additional smoothing is needed, and vice versa [29]. Sliding this function along the signal, it reflects the variations of the angle between the two segments. The movement of the segments resemble the wings of a butterfly, hence the name '***Wings***'.

Well-shaped negative peaks of '***Wings***' corresponded to every Q, R and S wave of the ECG signal. Negative peaks appeared also at the maximum slew rate of QR and RS segments. This is demonstrated in Fig. 4c, where the '***Wings***' function is shown as a thin line.

'***Wings***' is further smoothed by two-pass moving-averaging with a window of 50 ms (block 4 of Fig. 3). The 'two-pass' moving-averaging is performed twice in the same forward direction. The result is a negative wave (shown by a thick line in Fig. 4c), that responds to the wave frequency of the ECG signal.

Block 5 of Fig. 3 transfers the particular values of the '***Wings***' function into a window length '***wl***', over which the final Savitzky-Golay filter is applied. If *W* is the smoothed '***Wings***' and $\boldsymbol{W_{max}}$, $\boldsymbol{W_{min}}$ are its maximum and minimum values, the transfer formula to '***wl***', varying from $\boldsymbol{wl_{min}}$ to $\boldsymbol{wl_{max}}$, is:

$$wl = wl_{\min} - \frac{(wl_{\max} - wl_{\min})(W - W_{\min})}{W_{\max} - W_{\min}} \quad (4)$$

The values $\boldsymbol{wl_{min}}$ = 5 ms to $\boldsymbol{wl_{max}}$ = 75 ms in our first publications [29-31] were chosen to fulfill the 35 Hz cutoff filtering recommendations [16]. In order to keep undistorted the diagnostic high-frequency components of the ECG signal, and complying with the 2007 recommendations of the American Heart Association [12], we expanded '***wl***' from $\boldsymbol{wl_{min}}$ = -40 ms (to force negative values in QRS interval, in order not to filter the signal if ***wl*** < 2 ms) to $\boldsymbol{wl_{max}}$ = 100 ms [34], reaching $\boldsymbol{wl_{max}}$ = 200 ms, when used in electromyography [35, 36].

The '***Wings***' function and its transfer to '***wl***' is presented in Fig. 6. The thin line in the 2nd subplot of Fig. 6 is represented for the method of Christov and Daskalov, 1999 [29] and complies with the old recommendations for a 35 Hz cutoff of the low-pass filter [16].

The thicker trace of the subplot is illustration of the method of Christov et al. [34], and complies with the new recommendations for a higher than 150 Hz cutoff frequency of the low-pass filter [12]. No filtration is performed if '***wl***' < 2 ms, and this is the case for the whole QRS interval as shown with vertical dashed lines in Fig. 6. The upper boundary wl_{max} = 100 means that at low frequency ECG spectra the cutoff frequency is around *Fc* = 17 Hz.

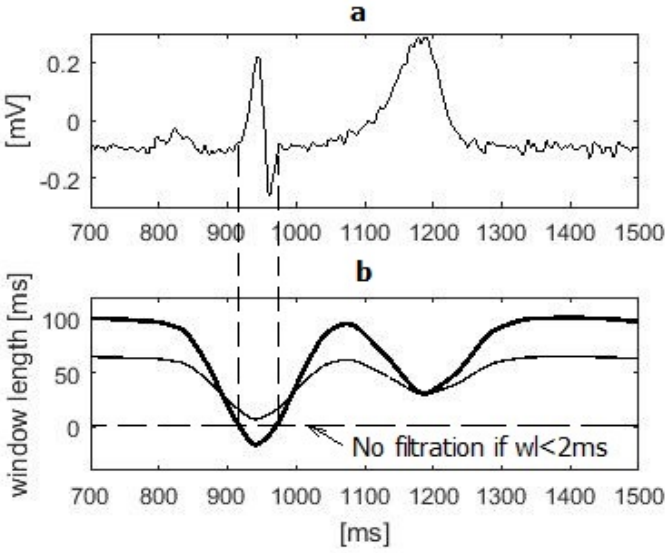

Fig. 6 '***Wings***' function and its transfer to window length '***wl***'.
Thin line is from Christov et al. [29]; thicker line is from Christov et al. [34].

Evaluation by the amount of filtered noise inside and outside the QRS-complex
The dynamic control was obtained by evaluation of the amount of filtered noise inside and outside the QRS-complex [31]. The method was not intended to work online since it needs preliminary location of the QRSon and QRSoff, performed by [40].

The retrieval of the Dynamic control, as well as the final filtering was based on the Savitzky and Golay [41] approximation procedure. The initial signal $\boldsymbol{X_i}$ was filtered ***n*** times with different lengths ***wl*** of the filtering window, to obtain ***n*** filtered signals $\boldsymbol{Y_i^n}$. Analysis of the difference between the original ECG signal $\boldsymbol{X_i}$ and the filtered one $\boldsymbol{Y_i^n}$ is made for every ***n*** by the standard deviation of residual noise inside QRS (std_RN_QRS) and outside QRS (std_RN_out):

$$\text{Std_RN_out}(n) = \text{std}\{Y_i^n - X_i\} \text{ for } i \text{ outside QRS interval,}$$
$$\text{Std_RN_QRS}(n) = \text{std}\{Yi^n - Xi\} \text{ for } i \text{ inside QRS interval.} \quad (5)$$

The ratio:

$$\text{r_in_out}\ (n) = \text{std_RN_out}(n) / \text{std_RN_QRS}(n) \quad (6)$$

is calculated ***n*** times, and the maximal value of ***n*** for which r_in_out(*n*) > 1 is considered as good value for filtering inside the QRS interval.

Inside the QRS interval, ***wl*** assumes its minimum value $\boldsymbol{wl_{min}}$ in the range from 8 ms to 24 ms, with a smooth transition towards outside the QRS, where it takes the maximum value of ***wl*** = 30 ms. The filtering algorithm modifies $\boldsymbol{wl_{min}}$ with decreasing values until the ratio r_in_out is > 1. The critical point of this kind of filter is the distortion inside the

QRS interval, and this is evident mainly with ECG signal with a low presence of high frequency noise.

Dynamic filtration
Ones the dynamic control has been evaluated, the actual filtering is done by:

- one-pass Savitzky-Golay filter [29, 31, 32, 35, 36],
- two-passes Savitzky-Golay filter [32, 33], or
- hybrid filtering – one-pass Savitzky-Golay filter at the QRSs intervals and transform-domain filtering elsewhere [30].

Approximation procedure of Savitzky-Golay
A smoothing procedure was adopted from Savitzky-Golay [41], a very general family of low pass filters, well-adapted for data smoothing. It performs an approximation by polynomial of grade ***m***, and makes use of the least squares approximation method, for defining the weighting coefficients. The mathematical description of the process is:

$$Y_i = \frac{1}{N} \sum_{j=-nR}^{j=nL} C_j X_{i+j}, \tag{7}$$

where ***Y*** and ***X*** represent the signal after and before approximation respectively, ***nL*** and ***nR*** – number of samples before and after the data point ***i***-th, C_j – weighted approximation coefficients, and ***N*** – a normalization coefficient, and both are depending on ***m***. The properties of SF family of low pass filetrs are discussed in Shafer [37]. The conditions for the optimal choice of SG filter are studied in Krishnan and Seelamantula [38].

The adopted smoothing procedure considers a quadratic polynomial approximation (***m*** = 2), and a symmetric approximation interval (***nL = nR = n***) for preserving the temporal structure of the time-varying signal. In this case, the procedure is applied on a window length ***wl*** of **2*n* + 1** samples, and the approximation and normalization coefficients are given by:

$$c_j = 3n^2 + 3n - 1 - 5j^2, \tag{8}$$

$$N = \frac{(2n+1)(4n^2+4n-3)}{3}. \tag{9}$$

Transform-domain method
We also used an EMG denoising by hybrid application of transform-domain method outside the QRS, and approximation methods in the QRS [29].

The ECG signal and the EMG noise were considered as vectors in a ***N***-dimensional signal space, namely ***s*** and ***e***, mixed additively to obtain the noisy signal, i.e.:

$$x = s + e \quad \text{for} \quad x, s, e \in \mathrm{R}^{\mathrm{N}}. \tag{10}$$

The EMG contamination can be assumed a short-term zero-mean Gaussian noise with variance $\boldsymbol{\sigma}^2$.

The idea was based on a temporal discrimination of the QRS-complexes (of higher-frequency and containing most of the signal energy) from areas outside the QRSs, characterized by

lower-energy and lower-frequencies. The discrimination rule is depending on the ECG signal slew rate. Different denoising techniques were applied on the two areas. In the segments outside the QRSs we aimed at an efficient EMG artifact suppression together with a preservation of some important small-amplitude details. This can be done by applying a transform domain denoising involving an appropriately selected transform domain coefficient shrinking threshold.

Applying a linear orthogonal transform ***T*** on Eq. (10), we get:

$$T(x) = T(s + e) = c + \varepsilon = y. \tag{11}$$

An appropriately chosen transform should compact the signal features into a small number of significant coefficients in **y,** while the noise would remain spread over all coefficients, being zero-mean Gaussian with variance $\boldsymbol{\sigma}^2$ in **ε**. An estimate of the noise-free signal can be obtained, applying a transform-domain filtering, in a form of a diagonal matrix

$$H = \text{diag}[h(1), h(2), \ldots, h(N)], \tag{12}$$

followed by the inverse transform,

$$s = T^{-1}HTx. \tag{13}$$

The idea of signal denoising by transform domain processing was popularized in a series of papers by Donoho and Johnstone developing an assortment of methods, summarized as *wavelet shrinkage* [42]. In their approaches, the considered transform ***T*** is the orthogonal wavelet transform and the operator ***H*** is a thresholding operator, realizing a hard or soft thresholding:

$$h(i) = \begin{cases} 1 & if \ |y(i)| > \tau \\ 0 & otherwise \end{cases}, \tag{14a}$$

$$h(i) = \begin{cases} 1 - \dfrac{\tau}{|y(i)} & if \ |y(i)| > \tau \\ 0 & otherwise \end{cases}. \tag{14b}$$

Most often the threshold τ is determined according to the universal threshold rule

$$\tau = \sigma\sqrt{2\ln M}, \tag{15}$$

where *M* is the signal length.

The wavelet shrinkage has shown good performance as asymptotically optimal in a minimax mean-squared-error sense. However, the decimation in the orthogonal decomposition causes shift-variance of the wavelet transform coefficients. This effect, combined with the coefficients thresholding, leads to some artifacts appearance. They can be avoided by applying a translation-invariant wavelet transform: an over-complete decomposition combining the decompositions of all shifted signal versions [43]. The inverse of this decomposition leads to multiple estimations of each signal sample to be averaged.

As an alternative to the neoteric wavelet transform, a discrete cosine transform (DCT) can be chosen. It possesses good energy compaction properties and has shown good performance, especially in processing highly correlated signals [44]. Some recent investigations have found DCT being superior in denoising of ECG signal and magnetic cardiogram signals [45, 46]. The translation-invariant paradigm can be realized by a sliding window DCT one sample at a time. The window size has to compromise between the requirements of sufficient temporal and frequency resolution.

Several forms of definition of the DCT exist [44]. One of most popular is the DCT type II that can be defined as:

$$c(k,n)=\begin{cases}\dfrac{1}{\sqrt{N}} & k=0 \quad 0\le n \le N-1 \\ \dfrac{2}{\sqrt{N}}\cos\dfrac{\pi (2n+1)k}{2N} & 1\le k\le N-1=0, \quad 0\le n\le N-1\end{cases}, \tag{16}$$

where $\boldsymbol{c(k, n)}$ is the $\boldsymbol{k}$-th and the $\boldsymbol{n}$-th element of the transform matrix $\boldsymbol{C}$ of size $\boldsymbol{N}\times\boldsymbol{N}$. The sliding DCT yields an over-complete decomposition $\boldsymbol{y = Tx}$, where $\boldsymbol{x}$ is the input signal vector of length $\boldsymbol{M}$, $\boldsymbol{T}$ is the block transform matrix, formed by the shifted versions of $\boldsymbol{C}$, and $\boldsymbol{y}$ is the output vector containing $\boldsymbol{M}\times\boldsymbol{N}$ transform coefficients (Fig. 7a). Actually, in order to place the transform window in the middle of the current sample and to have exactly $\boldsymbol{M}$ windows, we have to extend the signal with $\boldsymbol{N}$ samples around the borders.

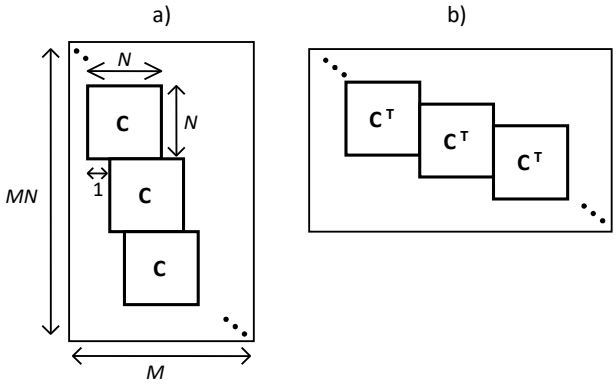

Fig. 7 (a) Decomposition block-matrix $\boldsymbol{T}$; (b) Reconstruction block matrix $\boldsymbol{T}^{\mathrm{T}}$.

Hence, every $\boldsymbol{N}$ successive samples in $\mathbf{y}$ represent the spectral coefficients for a given time instant. The decomposition can also be interpreted as an output of an $\boldsymbol{N}$-channel filter bank where the filters are formed by the reversed rows of the matrix $\boldsymbol{C}$. After some coefficient shrinkage, the inverse transform can be performed just by using the transposition of the matrix $\boldsymbol{T}$ (Fig. 7b) with some proper normalization (averaging), formally represented by a matrix $\boldsymbol{D}$:

$$x = DT^{\mathrm{T}}Hy. \tag{17}$$

Thus, we get for each sample an average of $\boldsymbol{N}$ estimations. Disadvantage of the transform-domain procedure is the significant consumption of time and computing resources.

Automatic on/off triggering of the filter

The EMG noise is not consistently present in the ECG signal. It may be absent entirely or be intermittent with different magnitude of the noise. For that reason, an automatic on/off triggering of the filter is an essential option. EMG noise has been successfully detected by Raphisak et al. [47], using morphological filters followed by QRS suppression. Automatic on/off triggering was applied and described in Christov et al. [33].

The block diagram of the automatic on/off triggering by Christov is presented in Fig. 8.

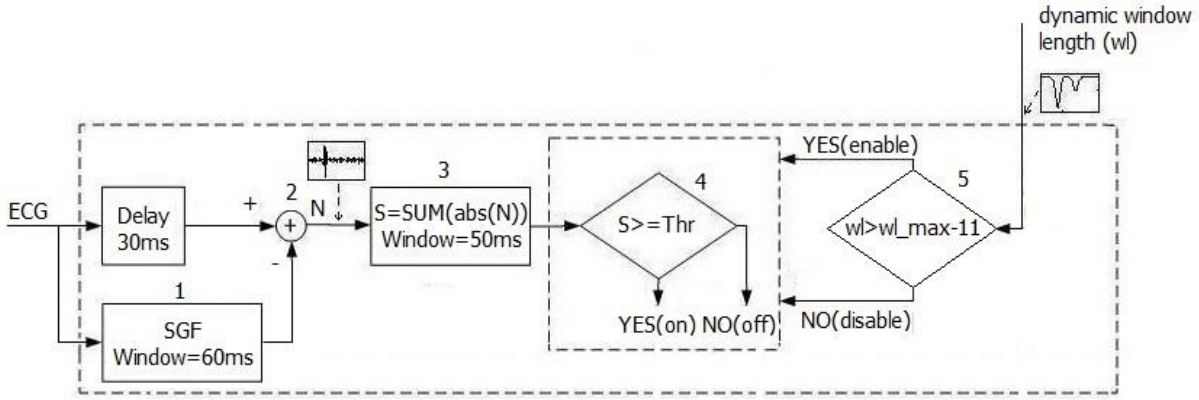

Fig. 8 Block diagram of automatic on/off triggering

The ECG signal was filtered initially by Savitzky-Golay within a fixed window of 60 ms. (block 1 of Fig. 8). This would suppress the high-frequency EMG noise, if it accompanies the ECG. Next few steps were to assess the presence/absence of noise: the raw ECG signal and the filtered one are subtracted (block 2 of the Fig. 8), *S* is the sum of all absolute values in a window of 50 ms which was calculated (block 3 of the Fig. 8), and then *S* was compared to a threshold value (block 4 of the Fig. 8). The result of this comparison controlled the on/off triggering of the filter. In order to avoid frequent switching, the turning-on was done after consecutive groups of noise indications in a period of 50 ms. In opposite, the turning-off was performed after consecutive noise-free indications in 100 ms. The turning-off condition was made more difficult because the ECG signal is usually accompanied by small EMG noise.

The above sequence would not work properly because the result of subtracting ECG – $ECG_{filtered}$ was strongly influenced by the filtering of the high frequency QRS components of the signal (Fig. 9c, see the dashed ellipse). Therefore, on/off triggering decision was made outside QRS, the indication of which is given by the decrease of '***wl***' with more than $\boldsymbol{wl_{max}}$ – **11** (block 5 of Fig. 8).

Real-time implementation

The final filtering in [33] is performed applying 2 times (2 passes) the time-linear smoothing procedure of Savitzky-Golay. Taking into account the maximal of ***wl*** = 65 ms, the actual filtering time is 2 × 65 ms = 130 ms.

The dynamic control of Fig. 5 is carried out over 220 ms: 60 ms for SGF, block 1 + 40 ms for FDF, block 2 + 20 ms for '***Wings***', block 3 + 100 ms for two-pass MAF, block 4.

The final filtering can be performed online with a delay of 350 ms.

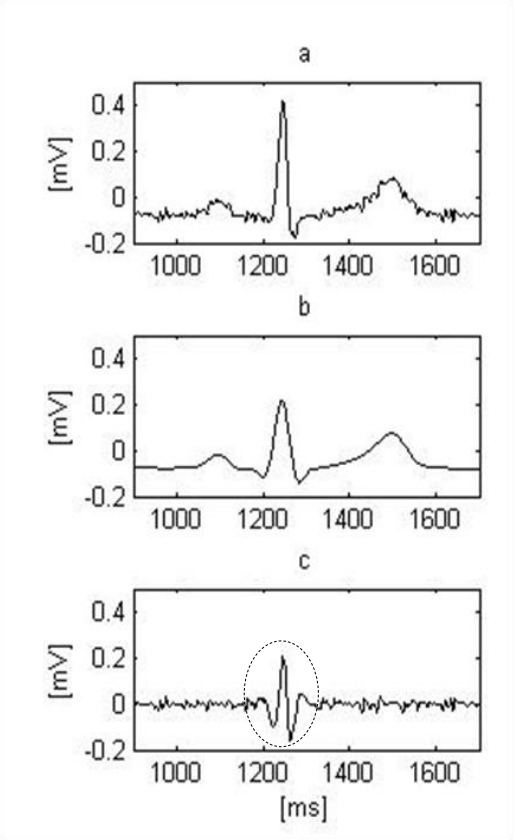

Fig. 9 (a) Raw ECG signal; (b) Filtered ECG signal; (c) $ECG_{raw} - ECG_{filtered}$.

Electromyography

Dynamic separation of ECG noise from EMG

Method of Dynamic separation of ECG from EMG was created to be used in electromyography [35]. We thought that once we successfully filtered the ECG, we would get a clean EMG only by subtracting this filtered the ECG from the input signal. Basically this was true, but with electrodes placed on the examined surface muscle, the amplitudes of the EMG signals, were equal or exceeding the amplitude of the ECG signal. Changes in the signal-to-noise ratio of the input ECG + EMG did not allow the direct use of the Dynamic filtration of ECG signal from EMG noise. Low filtration level of dynamic filtering window with ***wl*** < 15 ms at muscle load allowed not only ECG signal but also EMG signal to pass. On the other hand, low filtration during muscle rest would be good to be done throughout QRS complexes. This made us to add a new dynamic control obtained through the "Estimation of the EMG level".

The block diagram of the Dynamic separation of ECG from EMG as presented in [40] consists of five linear procedures:

1. Maximal suppression of power-line interference and EMG signal;
2. Assessment of '***Wings***' for evaluation of the frequency spectra of the ECG signal;
3. Estimation of the 'EMG level' used further for control of the minimal level of the dynamic filtration;
4. Dynamic filtration of the EMG signal from the initial signal with regard to the '***Wings***' and 'EMG level' aiming to achieve maximal preservation of the ECG signal;
5. Subtraction of the ECG signal from the input signal.

Estimation of the EMG level

The role of the EMG level estimation in the control of the ECG signal and EMG separation is shown in Fig. 10. Estimation of the EMG level was performed with the following equation:

$$L_i = \sum_{j=i-17ms}^{j=i+17ms} abs(In(j)),\ i > 17 \text{ ms}, \quad (16)$$

where ***In* = ECG + EMG** signal is the input signal presented at the first subplot of Fig. 10. The '***L***' estimator is controlling the window length '***wl***' of the Savitzky-Golay filter [41] only during QRS, not allowing ***wl* < *L*** (see Fig. 10c). The choice of 17 ms at equation 16 has been done empirically, aiming the '***L***' estimator to vary between 7 and 15 during rest and between 17 and 25 during muscle load.

Real-time implementation

Four of the five procedures of the method have a constant time execution window: power-line suppression (20 ms); EMG signal suppression (60 ms); evaluation by '***Wings***' of the number of samples in the filtering window (20 ms); estimation of the EMG level and subtraction of the ECG signal from the input signal (34 ms). Dynamic filtration is the only procedure having variable execution time, depending on the length of the filtering window '***wl***'. Taking into account that wl_{max} = 200 ms, the total execution window is less than 340 ms, which determines the time-delay of the pseudo-real-time mode.

Results

Electrocardiography

Databases

For the **ECG projects** [29-33] we used our digital ECG database of patients with renal disease [48] The ECGs (1- minute duration, 12-standard leads, 500 Hz sampling rate) were recorded before, and 3 minutes after a hemodialysis session.

EMG noise was obtained from two ECG electrodes placed on one forearm. ECG amplifier was used and the recordings (400 Hz sampling rate) were made during sustained voluntary effort. Both ECGs and EMGs signals were resampled to 1000 Hz. The artifacts were weighted and additively mixed with the different ECG signals subjected to processing.

Noise-free ECGs were obtained from the CTS ECG Test Atlas [49]. It contains artificially simulated ECG-like signals of different shapes. The so-called "analytical ECGs" are with shapes very close to the biological shapes, with QRS morphology like in real, normal ECG signals.

Noise suppression

The EMG noise suppression is demonstrated in Fig. 11. ECG signal with superimposed EMG noise with maximal value of around 0.1 mV is shown in the first subplot. The second subplot is a noise-free ECG signal as a result of the filtering procedure. It can be seen that the processed ECG signal has diagnostic capabilities even in the low-frequency zones such as P-waves, ST-segments, and T-waves. The difference between subplot 1 and subplot 2 (shown in subplot 3) is representing the EMG noise that has been suppressed.

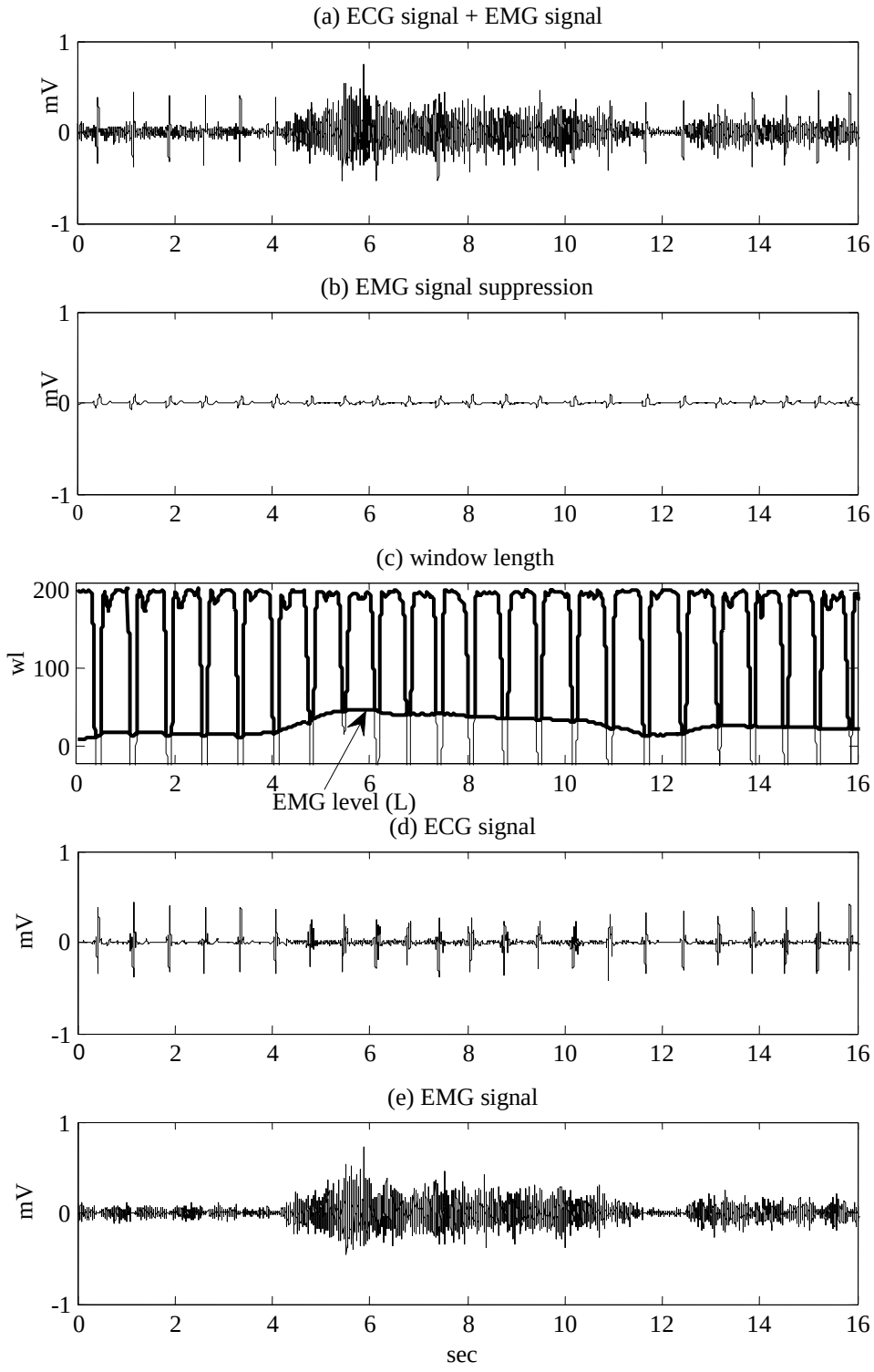

Fig. 10 Separation of ECG from EMG signal

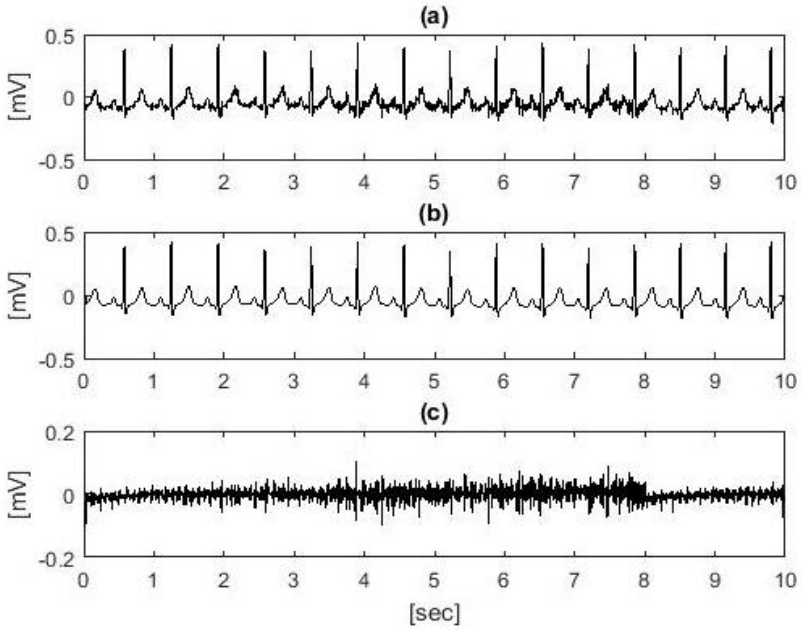

Fig. 11 Noise suppression: (a) Noisy ECG signal; (b) Filtered ECG signal;
(c) Suppressed EMG noise (first subplot minus second subplots).

As a result of the filtering, Fig. 11c contains not only the suppressed EMG signal but also ECG distortions. They are dozens of times less than the suppressed EMG noise, invisible to a naked eye and will be subject of attention later on.

Another example of EMG noise suppression is demonstrated in Fig. 12, where the 1st plot is real EMG signal, and the 2nd plot is the filtered EMG signal.

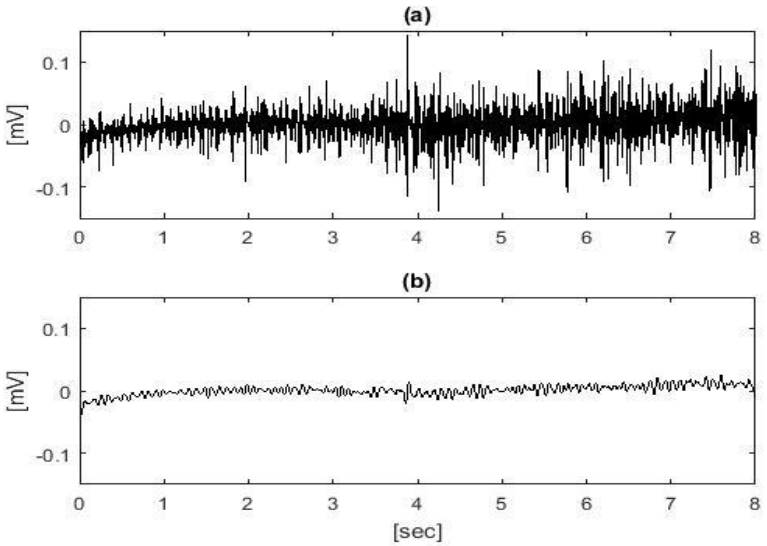

Fig. 12 Noise suppression:
(a) Real EMG noise recorded during sustained muscle effort;
(b) Filtered EMG signal.

Signal distortion

A noise-free ECG signal is shown in the first subplot of Fig. 13. Due to the fact that a noise-free ECG signal cannot be recorded in practice, simulated ECG-like signal obtained from the CTS ECG Test Atlas [48] was considered. The processed ECG signal is shown in

the second subplot. No distortions can be seen with naked eyes. However, at the enlarged scale of the third subplot, which presents the difference between the noise-free ECG signal and the processed one, distortion of around 0.06 mV, manifested as decrease of the QRS amplitude, can be observed.

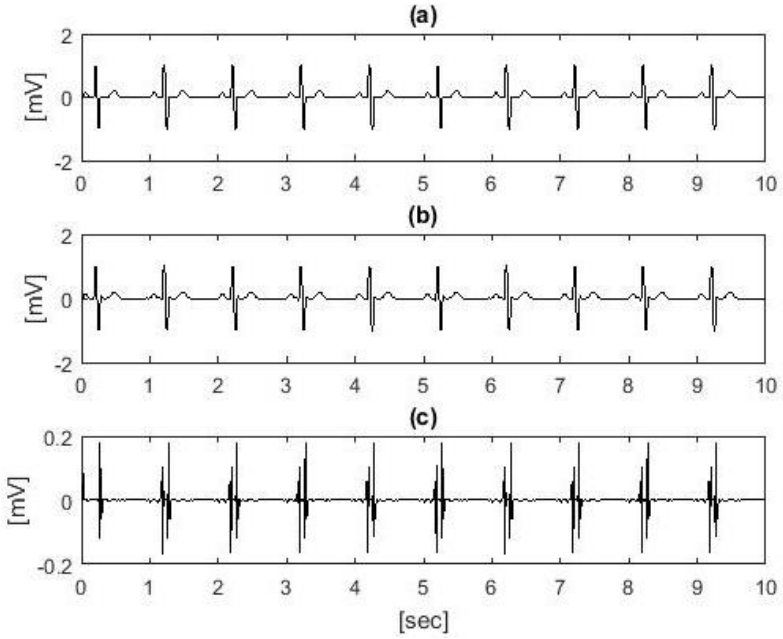

Fig. 13 Signal distortion: (a) Noise-free ECG signal, file ANE20000. IEC of the CTS ECG Test Atlas; (b) Processed ECG signal; (c) Signal distortion, ECG – ECG.

This decrease of QRS is around 6% of its amplitude. The root-mean-square error of distortion is RMS = 7.7 μV.

Quantitative assessment of the filtering efficiency

The filtering efficiency was quantitatively evaluated using conditionally clean ECG signals and typical disturbances to calculate the level of noise suppression *NS* by the initial disturbance n_{ini} mixed with the clean ECG signal and the residual disturbance n_{res} after filtering the contaminated signal

$$NS = \frac{n_{ini}}{n_{res}}. \tag{18}$$

Noise suppression is computed from root-mean-square (***rms***) values.

The quantitative assessment of the filtering efficiency was performed using the noise presented in Fig. 12a, mixed with the noise-free ECG signal of Fig. 13a.

Two values for noise suppression are calculated because of the non-homogeneous (dynamic) procedure: strong filtration of the low frequency components of the ECG signal as P-wave, PQ-interval, ST-interval, T-wave and TP-interval, and mild filtration of the high frequency QRS components.

$NS_{in\ QRS}$ = 3.3 dB, $NS_{out\ QRS}$ = 9.3 dB. (19)

On/off triggering

The distortion shown in Fig. 13 is theoretical, and will not be obtained in practice, due to switching-off of the filtering procedure in case of noise-free ECG signal. The block diagram and the on/off triggering algorithm were discussed in the previous chapter.

The triggering is demonstrated in Fig. 14. The first subplot is an ECG signal accompanied with bursts of EMG noise of different amplitudes within the intervals 1.0-4.0 sec, 8.0-12.0 sec, and 14.0-18.2 sec. The lower trace in subplot 1 is for the check whether $wl > wl_{max}$ – **11** (block 5 of Fig. 8). It is a peculiar indication of the occurrence of natural high-frequency signal as QRS and prevents erroneous decision for the presence of EMG noise and corresponding switching-on of the filter. The dashed line in subplot 1 of Fig. 8 indicates the on/off triggering.

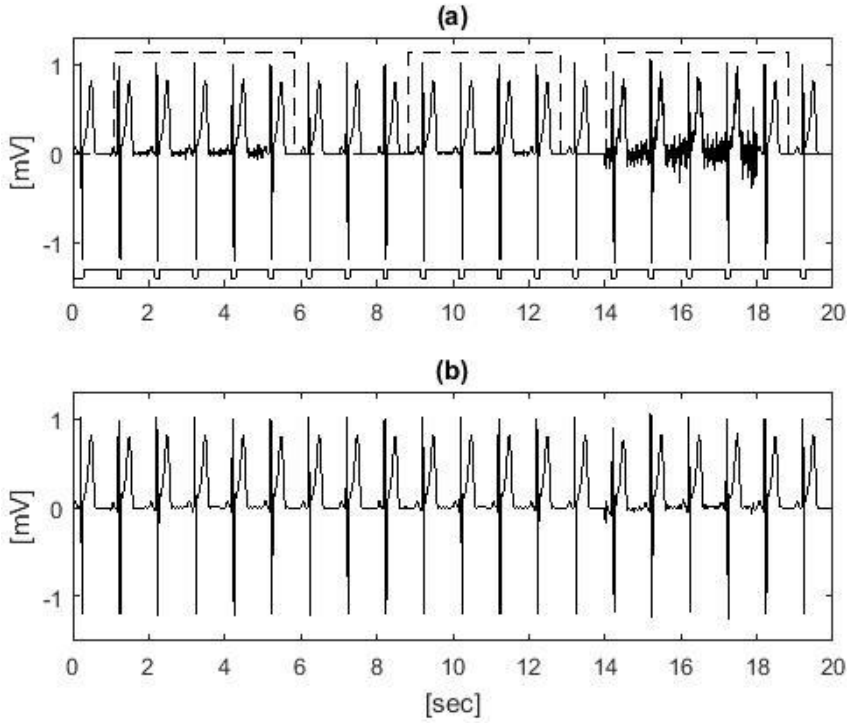

Fig. 14 On/off triggering: (a) Upper trace – ECG signal with bursts of noise, lower trace – indication of the occurrence of HF signal as QRS, dashed trace – on/off switching of the filter; (b) Processed signal.

The combined effect of filtering in case of noise, and no filtering in case of noise-free ECG signal, is shown in Fig. 14b.

Electromyography

Databases

For the **EMG projects** we used our digital database, fully described in [35]. The following muscles on the left side of the trunk were examined and recorded (1500 Hz, 1 min): deltoideus pars acromialis, pectoralis major and latisimus dorsi. Seven motor tasks were performed, aiming to register 3 different cases: low EMG signal to high ECG signal, low ECG signal to high EMG signal and an EMG and an ECG signal with almost equal amplitude.

Dynamic separation of ECG from EMG

The efficiency of the method was tested by comparison of:

- initial to final ECG signal (Fig. 15B and Fig. 15E), and
- initial to final EMG signal (Fig. 15A and Fig. 15F) using as a benchmark the power spectra obtained by Fast Fourier Transform (FFT).

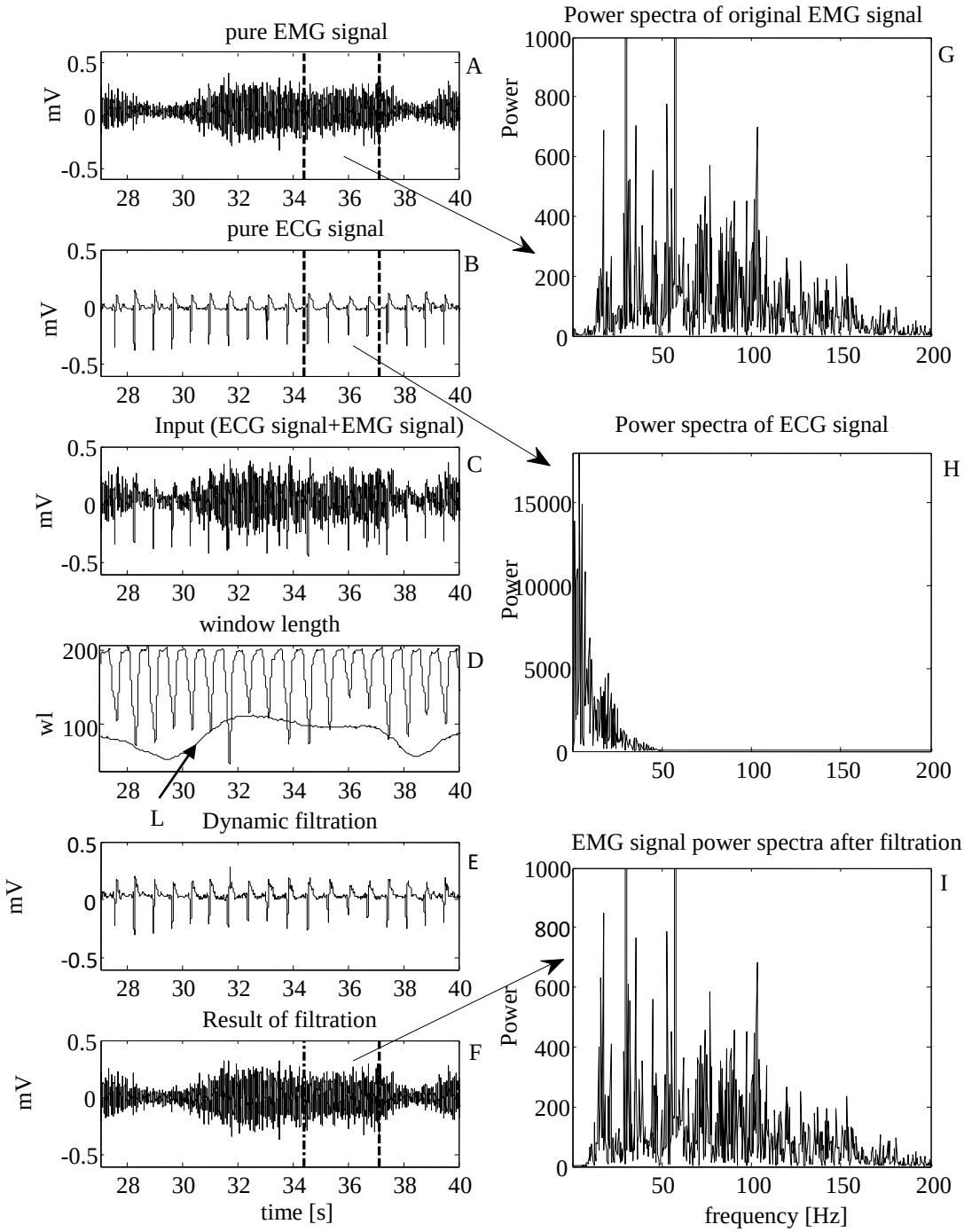

Fig. 15 Left: Successive steps of the algorithm in case when the amplitudes of the ECG signal and EMG signal were similar. Right: power spectra of the pure EMG signal and ECG signal as well as of the filtered EMG signal. Vertical dashed lines on the left mark the time interval where the FFT was performed.

Clear EMG signal of muscle DELacr (Fig. 15A) and clear ECG signal recorded at a place of the body with no muscle activity (Fig. 15B) were summed, and the signal presented in Fig. 15C was the object of the Dynamic separation. First, EMG signal was suppressed, then '***Wings***' function was developed and transferred to window length '***wl***' (Fig. 15D). As it can be seen, '***wl***' has low values at the high-frequency QRS components of the ECG signal, providing almost no filtration and, therefore minimal signal distortion. Outside QRS, maximal filtration was performed resulting in maximal suppression of the EMG signal. The signal ***L*** obtained by Eq. (16) limits the too low filtration at a high level of the EMG signal. ***L*** was considered only in cases of ***wl*** < ***L***. Savitzky and Golay approximation with dynamic change of the window length was applied to obtain a clear ECG signal (Fig. 15E). The ECG signal closely resembles the initial one shown in Fig. 15B. The final EMG signal was obtained by subtracting the filtered ECG signal (Fig. 15E) from the mixed signal (ECG + EMG) (Fig. 15C).

In order to test the efficacy of the method, we measured the RMS error between the initial and the estimated EMG signal. Two separate measurements were performed: in active muscle (where peak-to-peak of the EMG signal is equal to 2 mV) and in muscle rest (where the muscle was supposed to be inactive, so peak-to-peak of the EMG signal is equal to 0.2 mV). To test the effect of the SNR on the RMS error we added the ECG noise of five different QRS peak-to-peak amplitudes: 0.1 mV, 0.5 mV, 1 mV, 2 mV, 4 mV. The results can be seen in Table 1.

Table 1. Effect of ECG amplitude on RMS error during muscle rest and active muscle

ECG peak-to-peak, [mV]	0.1	0.5	1	2	4
RMS in active muscle, [mV]	0.0187	0.0161	0.0161	0.0160	0.0159
RMS in rest muscle, [mV]	0.0110	0.0119	0.0120	0.0120	0.0120

We observed an interesting phenomenon: in active muscle the RMS error between the initial and the estimated EMG signal was greatest at the lowest values of ECG noise. This was due to the fact that the method relies on good detection of cardiac activity which, at very low amplitudes, was difficult to achieve in the presence of an EMG signal, which was dozens of times stronger.

The closer the initial ECG signal and the filtered one are, the more successful the final result is. The initial and the filtered EMG signal (Fig. 15A and Fig. 15F) appear similar, but in order to prove that the EMG signal was not distorted by the procedure, we did a FFT. The power spectra from FFT using 4096 points (2.7 s) is shown on the right column of Fig. 15. The 2.7 s segment was depicted on Fig. 15A and 15B with vertical dashed lines. The great degree of convergence in the power spectra of the clear EMG signal (Fig. 15G) and the one obtained by dynamic filtration (Fig. 15I) was a proof for the good performance of the method.

Three parameters characterizing the power/frequency function were calculated: sum of the normalized power (S), mean frequency (MNF) and median frequency (MDF) [50]. For the power/frequency functions shown in Fig. 15G and Fig. 15I, these parameters were as follows: S = 44.96 arbitrary units, MNF = 90.10 Hz and MDF = 79.47 Hz for the original signal and S = 48.01 arbitrary units, MNF = 87.55 Hz and MDF = 76.54 Hz for the filtered signal. It has to be mentioned that the EMG signal was first normalized to the maximal values of its amplitude, recorded during maximal isometric tasks [39]. Both MNF and MDF

decreased after the filtration but the values were similar. It meant that the filtering did not destroy the signal, which is also visible in Fig. 15A and Fig. 15F.

Discussion

Electrocardiography

In the introduction, it was mentioned that the old (1967) recommendations for a low-pass filter of the American Heart Association was 35 Hz cutoff frequency [16], while the new (2007) recommendations were 150 Hz for adolescents and adults, and 250 Hz for children [12]. The effect of the filtering with cutoffs frequency of 35 Hz, 150 Hz and 250 Hz were shown in Fig. 1 and Fig. 2. No suppression of EMG was observed with low-pass filtering with cutoff frequencies of 150 Hz and 250 Hz, however there was no signal distortion in the HF band of the ECG (the QRS). Certain suppressions of the EMG signal could be seen with filtration with a cutoff frequency of 35 Hz. At the same time, there is a distortion, manifested as reduction of the QRS amplitude with 15% for the 1st, and 17% for the 2nd ECG signal of Fig. 1. Distortions were getting bigger with increase of the frequency spectrum.

The QRS segmentation, shown in the 2nd example of Fig. 1, which is indicative for an increased risk of sudden cardiac death decrease with > 300% in amplitude when processed with a cutoff frequency of 35 Hz. Frequency response of the dynamic filter is shown in Fig. 16. The cutoff frequency varies with the dynamic change of the window length of the Savitzky-Golay filter. As can be seen from Fig. 16c, the cutoffs are: from 13 Hz at the linear segments of the ECG signal, trough 25 Hz for the T-waves of high amplitude, and up to 400 Hz for the QRS-complexes.

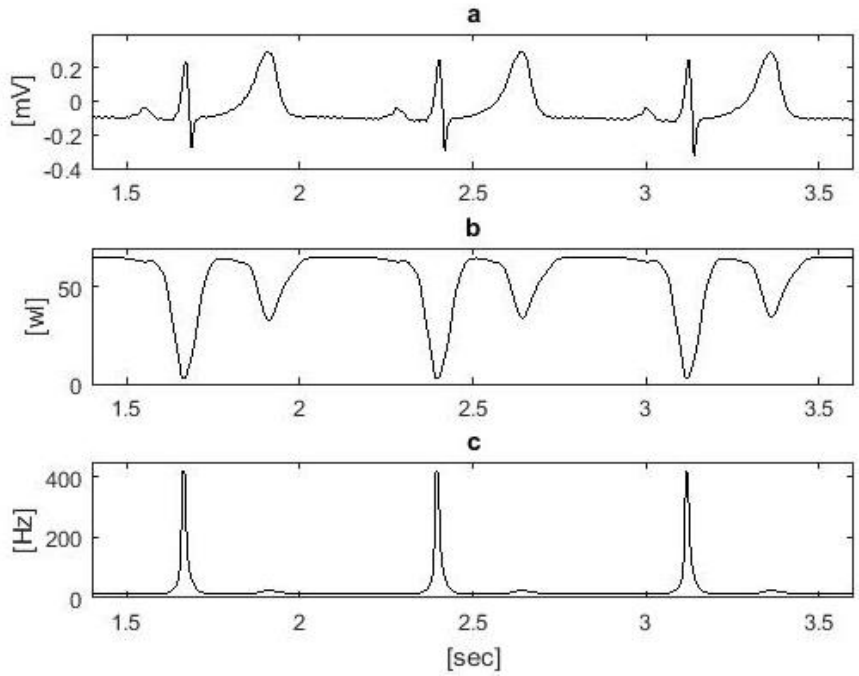

Fig. 16 Frequency response of the dynamic filter: (a) ECG signal; (b) Dynamic window length '***wl***' of the Savitzky-Golay filter; (c) Instantaneous cutoff frequency of the filter.

Electromyography

Removing the ECG signal is very important for injured people who may need orthesis controlled by EMG signals. Drake and Callaghan [5] conclude that a Butterworth high-pass filter with a 30 Hz cut-off frequency is the optimal balance between ease of implementation, time investment, and performance.

For that reason, we processed the experimental data of Fig. 17a with a 4^{th} order, high-pass Butterworth filter with cut-off frequency of 30 Hz. The suggested method based on dynamic filtration is separating the EMG signal from the ECG signal without EMG signal distortion across its entire frequency range regardless of the ECG signal amplitude (Fig. 17b). The Butterworth filter suppresses signals in the 0-30 Hz range, thus preventing the low-frequency analysis of the EMG signal.

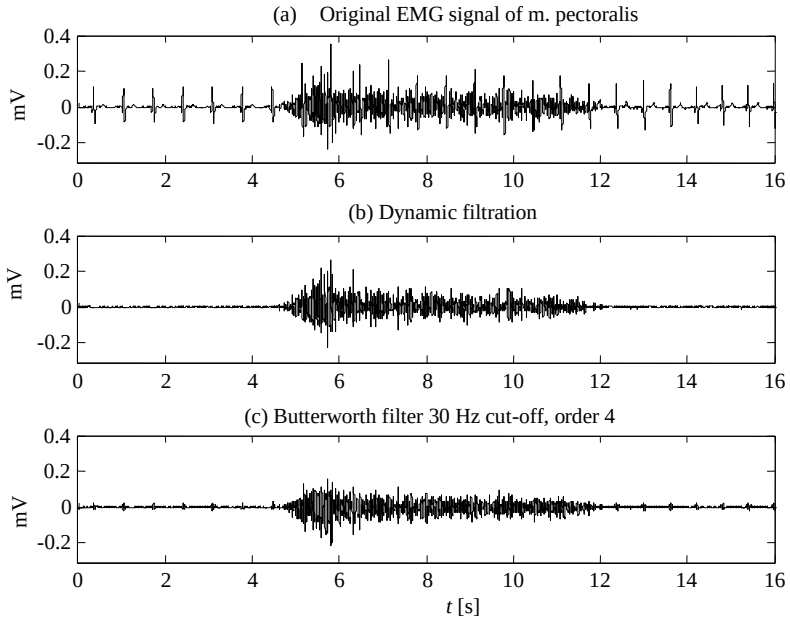

Fig. 17 Comparison of dynamic separation and Butterworth filtering

An additional disadvantage is that it passes high-frequency ECG signal components, which is apparent at equal and higher amplitudes of the ECG signal as compared to the EMG signal. This can be seen in the filtered by Butterworth signal (Fig. 17c) during muscle silence periods 0.4-4.5 s and 12.5-16 s.

It should be noted that the dynamics of '***wl***' is determined not by whether the muscle is in a period of EMG burst or in a silence. The dynamics is determined by the frequency spectra of the ECG, as can be seen in Fig. 16.

The method can be applied to cases of abnormal, arrhythmic ECG signal. It can also work with ECG signals shifted to higher frequency range higher than 200 Hz, for example in individuals with symptomatic QRS fragmentation, ECG signals of children, etc. An example is given in Fig. 18. The ECG recording shown in Fig. 19a were taken from the Physionet 2017 Challenge Database (https://physionet.org/challenge/2017/) and was superimposed with our recorded pure EMG signal (Fig. 18b). As can be seen from Fig. 18d, the algorithm works very well and removes ECG signal.

Muscle-rest periods are difficult to be detected by most known methods because of the high-amplitude ECG and the low signal-to-noise ratio. The processed by 30 Hz cutoff, 4th order, high-pass Butterworth filter, passes residual QRS of higher amplitudes (Fig 17c). Willigenburg et al. [7] and Lu et al. [8] mention that the effectiveness of their algorithms also depends on the signal-to-noise ratio.

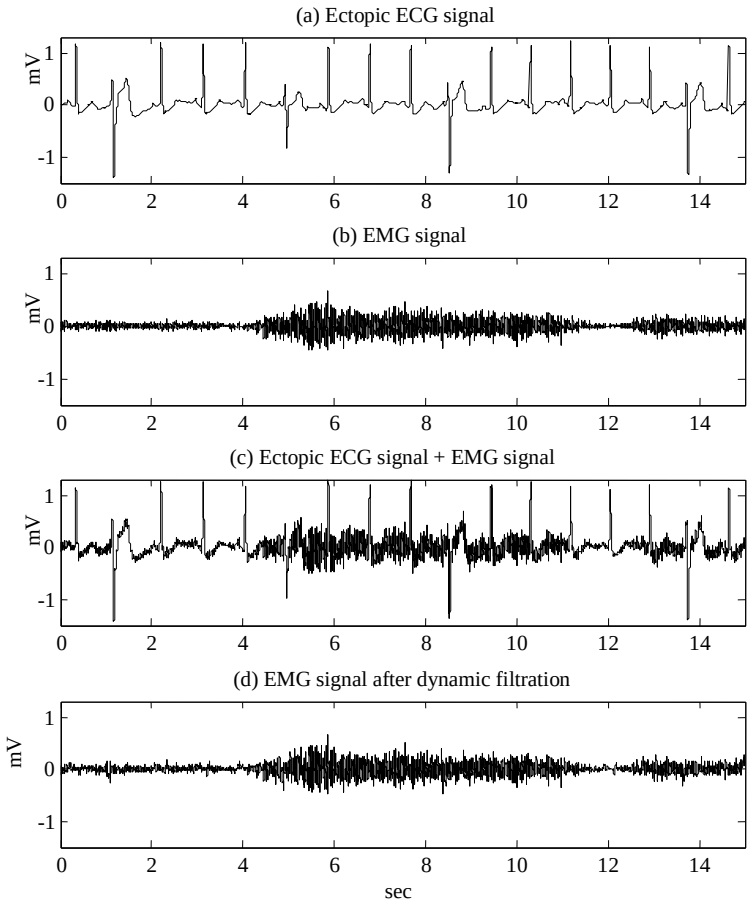

Fig. 18 Dynamic filtration of EMG signal from ECG noise
in case of ectopic beats in ECG

Contrary to filters in scientific literature, the suggested method shows better results at lower signal-to-noise ratio and vice versa (Table 1), due to the fact that it relies on good detection of cardiac activity which, at very low amplitudes, was difficult to achieve in the presence of an EMG signal, that was dozens of times stronger.

Investigating the EMG activities of the muscles of the upper limbs, Raikova et al. [39] found strong contamination of the EMG recordings by ECG noise. Fig. 19 is a visual presentation that an on/off control of an exoskeleton is impossible without elimination of the ECG noise, achieved by Dynamic separation of the two signals.

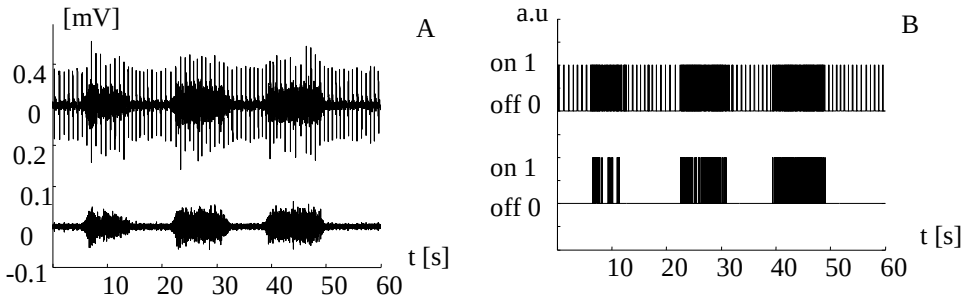

Fig. 19 Effects of filtration of the EMG signal:
A, up – EMG signal accompanied by strong ECG noise of the muscle pectoralis major;
A, down – Dynamic separation and subtraction of the ECG noise;
B – on/off control of an exoskeleton: up – improper, down – proper.

Conclusions

The conflicting requirements for a strong suppression of EMG noise in electrocardiography, and at the same time a maximal preservation of the ECG high-frequency components, prompted us to create in 1999 a Dynamic procedure, self-adjustable to the frequency spectra of the waves. The method allows the low-frequency components of the ECG signal as P-wave, PQ-interval, ST-interval, T-wave and TP-interval to be strongly filtered with a cutoff frequency of 14-40 Hz, while the high-frequency QRSs are mildly filtered with cutoff frequency of 100-500 Hz. The strong preservation of the signal's morphology improves the diagnostic capabilities of the ECG signal in the presence of EMG noise in both high- and low-frequency components. The method has been improved over the years with the ability to work online, and with automatic on/off triggering on whether or not there was electromyographic noise. The last revision of the method are consistent with the new AHA requirements (2007) for low-pass filtering of ECG with a cutoff frequencies of 150 Hz for adolescents and adults, and to 250 Hz for children.

The Dynamic procedure was modified to be used in electromyography, where the removal of ECG noise is imperative. The method consists in accepting that EMG is noise in the original ECG + EMG signal. Noise-free ECG is obtained by the Dynamic procedure and subtracted from the original signal to get a noise-free EMG.

References

1. Gopura R. A. R. C., K. Kiguchi, Y. Li (2009). SUEFUL-7: A 7DoF Upper-limb Exoskeleton Robot with Muscle-model-oriented EMG-based Control, IEEE/RSJ International Conference on Intelligent Robots and Systems, 1126-1131.
2. Kiguchi K., Y. Imada, M. Liyanage (2007). EMG-based Neuro-fuzzy Control of a 4DOF Upper-limb Power-assist Exoskeleton, Conf Proc IEEE Eng Med Biol Soc, 3040-3043.
3. De Luca C. J. (2002). Surface Electromyography: Detection and Recording, DelSys Inc., https://www.delsys.com/Attachments_pdf/WP_SEMGintro.pdf.
4. Merletti R. (1999). Standards for Reporting EMG Data, International Society of Electrophysiology and Kinesiology, http://people.stfx.ca/smackenz/courses/HK474/Labs/EMG%20Lab/isek_emg-standards.pdf.
5. Drake J. D. M., J. P. Callaghan (2006). Elimination of Electrocardiogram Contamination from Electromyogram Signals: An Evaluation of Currently Used Removal Techniques, Journal of Electromyography and Kinesiology, 16, 175-187.

6. Sbrollini A., A. Agostinelli, M. Morettini, F. Verdini, F. Di Nardo, S. Fioretti, L. Burattini (2017). Separation of Superimposed Electrocardiographic and Electromyographic Signals, In: European Medical and Biological Engineering Conference & Nordic-Baltic Conference on Biomedical Engineering and Medical Physics, June 11-15, Tampere, Finland, 518-521.
7. Willigenburg N. W., A. Daffertshofer, I. Kingma, J. H. van Dieën (2012). Removing ECG Contamination from EMG Recordings: A Comparison of ICA-based and Other Filtering Procedures, Journal of Electromyography and Kinesiology, 22, 485-493.
8. Lu G., J.-S. Brittain, P. Holland, J. Yianni, A. L. Green, J. F. Stein, T. Z. Aziz, S. Wang (2009). Removing ECG Noise from Surface EMG Signals Using Adaptive Filtering, Neuroscience Letters, 462, 14-19.
9. Zhou P., B. Lock, T. A. Kuiken (2007). Real Time ECG Artifact Removal for Myoelectric Prosthesis Control, Physiol Meas, 28, 397-413.
10. Abbaspour S., A. Fallah (2014). Removing ECG Artifact from the Surface EMG Signal Using Adaptive Subtraction Technique, J Biomed Phys Eng, 4(1), 33-38.
11. Christov I., T. Dobreva, R. Raikova (2019). ECG-noise Removal from EMG-signal by Subtraction of Hybrid Template of Averaged PQRS-T Intervals, 2019 IEEE XXVIII International Scientific Conference Electronics (ET), doi: 10.1109/ET.2019.8878620.
12. Kligfield P., L. S. Gettes, J. J. Bailey, R. Childers, B. J. Deal, E. W. Hancock, G. van Herpen, J. A. Kors, P. Macfarlane, D. M. Mirvis, O. Pahlm, P. Rautaharju, G. S. Wagner, M. Josephson, J. W. Mason, P. Okin, B. Surawicz, H. Wellens (2007). Recommendations for the Standardization and Interpretation of the Electrocardiogram: Part I: The Electrocardiogram and Its Technology. A Scientific Statement from the American Heart Association Electrocardiography and Arrhythmias Committee, Council on Clinical Cardiology; the American College of Cardiology Foundation; and the Heart Rhythm Society Endorsed by the International Society for Computerized Electrocardiology, J Am Coll Cardiol, 49, 1109-1127.
13. Dotsinsky I., I. Christov, I. Daskalov (1996). Assessment of Metrological Characteristics of Digital Electrocardiographs, J Clin Eng, 21, 156-160.
14. García-Niebla J., G. Serra-Autonell (2009). Effects of Inadequate Low-pass Filter Application, J Electrocard, 42(4), 303-304.
15. Nakagawa M., C. Tsunemitsu, S. Katoh, Y. Kamiyama, N. Sano, K. Ezaki, H. Miyazaki, Y. Teshima, K. Yufu, N. Takahashi, T. Saikawa (2014). Effect of ECG Filter Settings on J-waves, J Electrocard, 47(1), 7-11.
16. Recommendation for Instruments in Electrocardiography and Vectorcardiography (1967). Subcommittee on Instrumentation Committee on Electrocardiography – American Heart Association, IEEE Tr BioMed Eng, 14, 60-68.
17. Das M. K., D. P. Zipes (2009). Fragmented QRS: A Predictor of Mortality and Sudden Cardiac Death, Heart Rhythm, 6(3), S8-S14.
18. Kligfield P., P. M. Okin (2007). Prevalence and Clinical Implications of Improper Filter Settings in Routine Electrocardiography, Am J Cardiol, 99, 711-713.
19. Sayyad R. A., K. Mundada (2016). Enhancement and Denoising of ECG Signal Using Extended Kalman Filter and Extended Kalman Smoother, J Innov Electronics Commun Eng, 6(1), 22-26.
20. Rakshit M., S. Das (2018). An Efficient ECG Denoising Methodology Using Empirical Mode Decomposition and Adaptive Switching Mean Filter, Biomed Sign Proc Contr, 40, 140-148.
21. Dotsinsky I., J. Mihov (2008). Tremor Suppression in ECG, Bio Med Eng OnLine, 7, 29, https://biomedical-engineering-online.biomedcentral.com/articles/10.1186/1475-925X-7-29.

22. Dotsinsky I., G. Mihov (2010). Simple Approach for Tremor Suppression in Electrocardiograms, Int J Bioautomation, 14(2), 129-136.
23. Joy J., P. Manimegalai (2013). Wavelet Based EMG Artifact Removal from ECG Signal, J Eng Comp & Applied Sci, 2(8), 55-58.
24. Tulyakova N. (2017). Locally-adaptive Myriad Filters for Processing ECG Signals in Real Time, Int J Bioautomation, 21(1), 4-18.
25. Tulyakova N., T. Neycheva, O. Trofymchuk, O. Stryzhak (2018). Locally-adaptive Myriad Filtration of One-dimensional Complex Signal, Int J Bioautomation, 22(3), 275-296.
26. De Pinto V. (1992). Filters for the Reduction of Baseline Wander and Muscle Artifact in the ECG, J Elòectrocard, 25, 40-48.
27. Kalra A., A. Lowe, A. Al-Jumaily (2018). Critical Review of Electrocardiography Measurement Systems and Technology, Meas Sci Techn, 30(1), 012001.
28. Luo S., P. Johnston (2010). A Review of Electrocardiogram Filtering, J Electrocard, 43, 486-496.
29. Christov I. I., I. K. Daskalov (1999). Filtering of Electromyogram Artifacts from the Electrocardiogram, Med Eng & Phys, 21(10), 731-736.
30. Gotchev A., I. Christov, K. Egiazarian (2002). Denoising the Electrocardiogram from Electromyogram Artifacts by Combined Transform-domain and Dynamic Approximation Method, Int Conf Acoustics, Speech and Signal Processing, ICASSP2002, Orlando, USA, May 13-17, 3872-3875.
31. Bortolan G., I. Christov (2014). Dynamic Filtration of High-frequency Noise in ECG Signal, Comput Card, 41, 1089-1092.
32. Bortolan G., I. Christov, I. Simova, I. Dotsinsky (2015). Noise Processing in Exercise ECG Stress Test for the Analysis and the Clinical Characterization of QRS and T Wave Alternans, Biomed Signal Process and Control, 18, 378-385.
33. Christov I., T. Neycheva, R. Schmid, T. Stoyanov, R. Abächerli (2017). Pseudo Real-time Low-pass Filter in ECG, Self-adjustable to the Frequency Spectra of the Waves, Med & Biol Eng & Comput, 55(9), 1579-1588.
34. Christov I., T. Neycheva, R. Schmid (2017). Fine Tuning of the Dynamic Low-pass Filter for Electromyographic Noise Suppression in Electrocardiograms, Comp in Card, 44, 1-4.
35. Christov I., R. Raikova, S. Angelova (2018). Separation of Electrocardiographic from Electromyogtaphic Signals Using Dynamic Filtration, Med Eng Phys, 57, 1-10.
36. Christov I., S. Angelova, R. Raikova (2018). Dynamic Procedure for Separation of Electromyographic and Electrocardiographic Recordings of Trunk Muscles, 27th Int Conf on Automation of Discreet Production, June 21-24, Sozopol, 202-207.
37. Schafer R. W. (2011). What is a Savitzky-Golay Filter? IEEE Sign Proc Mag, 28(4), 111-117.
38. Krishnan S. R., C. S. Seelamantula (2013). On the Selection of Optimum Savitzky-Golay Filters, IEEE Trans Sign Process, 61, 380-391.
39. Raikova R., S. Angelova, I. Veneva, I. Christov (2019). Experimental Investigation of Electromyographic Activities of Upper Limb Muscles without and with a Passive Exoskeleton with Four Degrees of Freedoms, Int J Bioautomation, 23(3), 343-354.
40. Degani R., G. Bortolan (1990). Methodology of ECG Interpretation in the Padova Program, Methods of Information in Medicine, 29, 386-392.
41. Savitzky A., M. Golay (1964). Smoothing and Differentiation of Data by Simplified Least Squares Procedures, Anal Chem, 36, 1627-1639.
42. Donoho D. L., I. Johnstone (1995). Adapting to Unknown Smoothness via Wavelet Shrinkage, J Amer Stat Assoc, 90, 1200-1224.

43. Coifman R., D. Donoho (1995). Translation-invariant De-noising, In: Wavelets and Statistics, Antoniadis A. (Ed.), Lecture Notes in Statistics, 103, 125-150.
44. Rao A., P. Yip (1990). Discrete Cosine Transform: Algorithms, Advantages, Applications, Academic Press.
45. Öktem R., L. Yaroslavsky, K. Egiazarian (1998). Signal and Image Denoising in Transform Domain and Wavelet Shrinkage: A Comparative Study, Proc of the 9th European Signal Processing Conference – EUSIPCO'98, Rhodes, Greece, September 8-11, 2269-2272.
46. Öktem H., K. Egiazarian, J. Nousiainen (1999). Local Adaptive De-noising Techniques in Transform Domain for EMCG De-noising, Proc of the Int Conf Acoustics, Speech and Signal Processing – ICASSP'99, March 15-19, Phoenix, Arizona, USA, 1769-1772.
47. Raphisak P., S. C. Schuckers, A. J. Curry (2004). An Algorithm for EMG Noise Detection in Large ECG Data, Comp in Card, 31, 369-372.
48. Simova I., I. Christov, L. Kambova, G. Bortolan, T. Katova (2014). QRS and T Loops Area Changes during Haemodialysis, Comput Cardiol, 41, 409-412.
49. Zywietz Chr. (1999). CTS-ECG Test Atlas, Center for Computer Electrocardiography. Biosignal Processing, Medical School, European Conformance Testing Services for Computerized Electrocardiography, Hannover, Germany.
50. Phinyomark A., S. Thongpanja, H. Hu, P. Phukpattaranont, C. Limsakul (2012). The Usefulness of Mean and Median Frequencies in Electromyography Analysis, Computational Intelligence in Electromyography Analysis – A Perspective on Current Applications and Future Challenges, Naik G. R. (Ed.), 195-220.

Prof. Ivaylo Christov, D.Sc.
E-mail: Ivaylo.Christov@biomed.bas.bg

Ivaylo Christov, M.Sc., Ph.D., D.Sc., has graduated as Electronic Engineer at the Technical University, Sofia. His Ph.D. thesis was on ECG acquisition and processing. His D.Sc. thesis was on ECG processing, automatic wave detection, automatic analysis and diagnosis. He is currently a Research Professor at the Institute of Biophysics and Biomedical Engineering, Bulgarian Academy of Science (IBPhBME – BAS). He is a member of the Working Group on e-Cardiology of the European Society of Cardiology. He was awarded as "Top Referee of the Year" and "Excellence in Reviewing" of several journals in the field of Biomedical Engineering. In 2013 he was awarded as "Scientific Excellence" of the Union of Scientists in Bulgaria.

Prof. Atanas Gotchev, D.Sc.
E-mail: atanas.gotchev@tuni.fi

Atanas Gotchev received the M.Sc. degree in Radio and Television Engineering in 1990 and in Applied Mathematics in 1992, and the Ph.D. degree in Telecommunications in 1996, all from Technical University of Sofia, Sofia, Bulgaria, and the D.Sc. (Tech.) degree in Information Technologies from Tampere University of Technology, Tampere, Finland, in 2003. Currently, he is a Professor of Signal Processing at the Unit of Computing Sciences and Director of the Centre for Immersive Visual Technologies, Tampere University. His research interests include sampling and interpolation theory, and spline and spectral methods with applications to multidimensional signal analysis. His recent work concentrates on algorithms for multi-sensor 3-D scene capture, transform-domain light-field reconstruction, and Fourier analysis of 3-D displays.

Prof. Giovanni Bortolan, Ph.D.
E-mail: giovanni.bortolan@isib.cnr.it

Giovanni Bortolan, laurea degree from the University of Padova, Italy in 1978, is a Senior Researcher at the Institute of Neuroscience of the Italian National Research Council (IN-CNR). He has published numerous papers in the area of medical informatics and applied fuzzy sets. He is actively pursuing research in medical informatics in computerized electrocardiography, neural networks, fuzzy sets, data mining, pattern recognition and biomedical signal processing.

Senior Assis. Prof. Tatyana Neycheva, Ph.D.
E-mail: tatiana@biomed.bas.bg

Tatyana Neycheva, M.Sc., Ph.D., has graduated as Electronic Engineer in Telecommunications at the Technical University, Sofia. Her Ph.D. thesis was on fast recovery defibrillator amplifiers and ECG signal processing after defibrillation shock. She is currently a Senior Assistant Professor at the IBPhBME – BAS, and is experienced in biomedical signal processing and firmware development for embedded microcontroller systems.

Prof. Rositsa Raikova, D.Sc.
E-mail: rosi.raikova@biomed.bas.bg

Rositsa Raikova was born in Shoumen, Bulgaria on 16 October, 1955. She received her Ph.D. in Biomechanics in 1993. She then worked in the Institute of Mechanics and Biomechanics at the Bulgarian Academy of Sciences. Now she is a Professor at the IBPhBME – BAS and a Head of the Department "Motor Control". Her research interests are in the field of biomechanics and motor control of the human limbs.

Ramun Schmid, Ph.D.
E-mail: Ramun.Schmid@schiller.ch

Ramun Schmid received his B.Sc. degree in Electrical Engineering in 2008 and his M.Sc. degree in 2010 from the University of Applied Sciences of Eastern Switzerland (FHO) with a main focus on digital signal processing. From 2010 to 2011 he was with the Institute for Communication Systems (ICOM) in Rapperswil, Switzerland, and since 2011 he is with the Signal Processing Group of SCHILLER AG, Baar, Switzerland.

© 2020 by the authors. Licensee Institute of Biophysics and Biomedical Engineering, Bulgarian Academy of Sciences. This article is an open access article distributed under the terms and conditions of the Creative Commons Attribution (CC BY) license (http://creativecommons.org/licenses/by/4.0/).